

1,2-Hydrogen Migration to a Saturated Ruthenium Complex via Reversal of Electronic Properties for Tin in a Stannylene-to-Metallostannylene Conversion

Hsueh-Ju Liu,[†] Julie Guihaumé,[‡] Thomas Davin,[‡] Christophe Raynaud,^{‡,§,||} Odile Eisenstein,^{*,‡} and T. Don Tilley^{*,†}

[†]Department of Chemistry, University of California, Berkeley, Berkeley, California 94720-1460, United States

[‡]Institut Charles Gerhardt, CNRS UMR 5253, Université Montpellier 2, F-34095 Montpellier, France

[§]UMR 7616, Laboratoire de Chimie Théorique, Sorbonne Universités, UPMC Univ Paris 06, F-75005 Paris, France

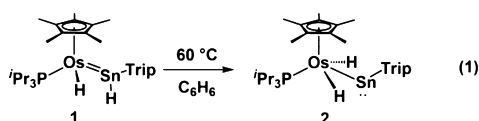
^{||}CNRS, UMR 7616, Laboratoire de Chimie Théorique, F-75005 Paris, France

S Supporting Information

ABSTRACT: An intramolecular 1,2(α)-H migration in a saturated ruthenium stannylene complex, to form a ruthenostannylene complex, involves a reversal of the role for a coordinated stannylene ligand, from that of an electron donor to an acceptor in the transition state. This change in the bonding properties for a stannylene group, with a simple molecular motion, lifts the usual requirement for generation of an unsaturated metal center in migration chemistry.

The 1,2-shift of hydrogen from a donor atom to a metal center (α -H migration) is a fundamental step in organotransition-metal chemistry that facilitates the formation of a variety of metal–ligand multiple-bonded species, including carbene, imido, oxo, and phosphinidene complexes.^{1–9} This migration usually requires an electronically unsaturated metal center that utilizes an empty acceptor orbital for activation of the α -substituent and for formation of the new metal–hydrogen bond. This laboratory has employed such migrations to synthesize carbene congeners of heavier group 14 atoms, including silylene,^{10–13} germylene,^{14–16} and stannylene¹⁷ complexes. For example, a cationic platinum silylene complex was generated via methide abstraction from (dippe)PtMe-(SiHMe₂) by B(C₆F₅)₃, presumably by way of a putative three-coordinate platinum species whose open coordination site allows 1,2-hydrogen migration from silicon to platinum.¹⁰

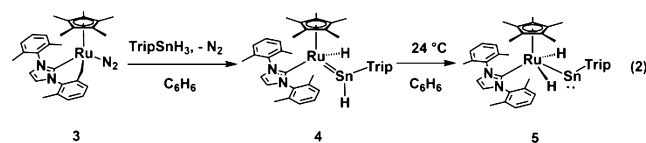
A fundamentally different type of α -H migration has recently been identified, involving a saturated metal center without an empty acceptor orbital. This process, until now, is associated only with the example shown in eq 1, involving isomerization of



the electronically *saturated* stannylene complex **1** to a metallostannylene complex (**2**; Trip = 2,4,6-*i*-Pr₃C₆H₂).¹⁷ In this case, experimental evidence suggests that the reaction is not intramolecular but is catalyzed by an adventitious radical

species. Thus, the reaction is zero-order with respect to the concentration of **1** and inhibited by radical traps (^tBu₃SnH or 9,10-dihydroanthracene). Here we describe a second example of this type of migration involving an analogous ruthenium system and present experimental and computational results that provide key insights into how such migrations can also occur by a simple, intramolecular process.

Metallo-yene complexes such as **2** are interesting, potential intermediates in new main group-based transformations, but few have been reported or studied in detail. The first examples were prepared by a salt-elimination reaction, involving a divalent R–E–Cl (E = Sn or Ge) compound and a nucleophilic and anionic complex containing a group VI metal (Cr,^{18,19} Mo,¹⁹ W^{18,19}), iron,^{20–22} or manganese.²³ The transformation of eq 1 represents a new pathway to metallo-yenes, which may allow the use of such species in metal-mediated processes that start from tetravalent main group starting materials (e.g., stannanes, germanes, and silanes, as in eq 2). The discovery of the first ruthenium metallostannylene, and an understanding of the chemistry associated with its formation (*vide infra*), should promote advances in this area.



A recently described synthon expected to provide access to metal-element doubly bonded species is the cyclometalated complex Cp**Ru*(IXy-H)N₂ (**3**, IXy = 1,3-bis(2,6-dimethylphenyl)imidazol-2-ylidene; “IXy-H” is the deprotonated form of IXy; Cp* = η^5 -C₅Me₅), which activates two Si–H bonds of a primary silane RSiH₃ via a rapid sequence of N₂ dissociation, Si–H oxidative addition, C–H bond elimination, and finally α -H migration to generate Cp*(IXy)(H)Ru=SiHR silylene complexes.²⁴ These results suggested that a Ru stannylene complex could be synthesized by reaction of **3** with a primary stannane, especially given the fact that Sn–H

Received: July 31, 2014

Published: September 23, 2014

bonds are weaker (and easier to activate) than comparable Si–H bonds. Indeed, reaction of **3** with 1 equiv of TripSnH_3 in benzene- d_6 instantly resulted in a color change from deep brown to deep green. The ^1H NMR spectrum of the reaction mixture reveals quantitative conversion of **3** to a new product **4** (eq 2), which features a downfield resonance at δ 16.2 ppm and a hydride resonance at δ –11.7 ppm. This spectrum, and in particular the downfield SnH resonance, suggests that the product is a stannylenne complex analogous to **1** (see Supporting Information (SI)). Attempts to isolate pure, solid samples of **4** were unsuccessful, due to its facile and quantitative conversion to a new, dark red species (**5**, eq 2).

The decay of **4** was monitored by ^1H NMR spectroscopy, which revealed that the conversion of **4** to **5** was complete after 2 h. The ^1H NMR spectrum of **5** indicates that the SnH hydrogen of **4** was replaced by a hydride ligand, given the presence of a new, singlet resonance at δ –9.5 ppm ($^1J_{\text{SnH}}$ 257.4 Hz), assigned to two Ru hydrides. Unfortunately, repeated attempts to use 1D or 2D NMR spectroscopy to observe a ^{119}Sn resonance were unsuccessful. Cooling a concentrated pentane solution of **5** at –30 °C afforded purple crystals in 85% yield, and X-ray crystallography clearly demonstrated that **5** is the first isolated Ru metallostannylenne complex, which features a Ru-bound, two-coordinate Sn center with a Ru–Sn bond of 2.660(1) Å and a Ru–Sn–C_{isop} bond angle of 106.1(2)° (Figure 1). These data are in good agreement with Pandey's prediction²⁵ that a phosphine-based Ru metallostannylenne complex should be stable.

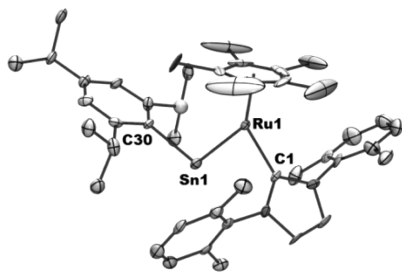


Figure 1. Molecular structure of **5** displaying thermal ellipsoids at the 50% probability level. H atoms have been omitted for clarity.

The transformation of **4** to **5** is unusual due to the apparent absence of an empty orbital at Ru to participate in the α -H migration. Therefore, a series of kinetics experiments were conducted to better understand the mechanism of this conversion. First, well-behaved kinetics were observed to ca. 90% conversion of **4** to **5**, and the rate exhibits a first-order dependence on [**4**]. Thus, the mechanism is distinct from that associated with the Os stannylenne system of eq 1, which exhibits a zero-order dependence on [**1**].¹⁷ Second, the observed KIE for the isomerization of eq 2, $k_{\text{H}}/k_{\text{D}} = 1.3$, suggests that Sn–H migration is involved in the rate-determining step. In addition, isolation of the reaction system from ambient light led to the same reaction rate, which was also unaffected by addition of a radical initiator (AIBN, benzene- d_6 , 0.5 equiv) or a radical inhibitor (9,10-dihydroanthracene or 2,6-di-*t*-butyl-4-methylphenol, benzene- d_6 , 10 equiv). Similarly, proton sponge (1,8-bis(dimethylamino)naphthalene, 10 equiv) or free IXy (5 equiv) did not significantly influence the conversion rate. These results are consistent with a unimolecular transformation of **4** to **5** without assistance by other species. The activation parameters for the isomerization are $\Delta H^\ddagger = 20.43 \pm 0.38$ kcal mol^{–1} and $\Delta S^\ddagger = -3.49 \pm 1.29$ cal mol^{–1} K^{–1}, as determined from an Eyring plot and rate constants obtained between 283 and 303 K (see SI).

DFT calculations²⁶ were performed to determine the reaction pathway for the formation of **5**. To distinguish between the experimental and the computed species, roman numerals are used for the latter. This level of calculations accurately reproduces the structure of **5**. The formation of **IV** starts with a thermodynamically favorable oxidative addition of a Sn–H bond of TripSnH_3 to **I** (the species resulting from N_2 dissociation from **3**),²⁴ with no detectable activation barrier (Figure 2). This process yields a four-legged piano stool structure with either H or SnH_2Trip *cis* to the metalated Ru–C bond, as illustrated by **II** and **VI**, respectively. The isomer **II** is less stable by 6.9 kcal mol^{–1}, and this might be attributed to the *trans* relationship of the metalated carbon and the stannyl group. However, **II** provides a low-energy pathway for reductive elimination of the metalated carbon with the hydride ligand, which requires an activation barrier of only 5.5 kcal mol^{–1} and results in the 16-electron Ru(II) complex that is 1.9 kcal mol^{–1} more stable than **II**. The presence of an empty coordination site at Ru in **III** allows for a facile α -H migration

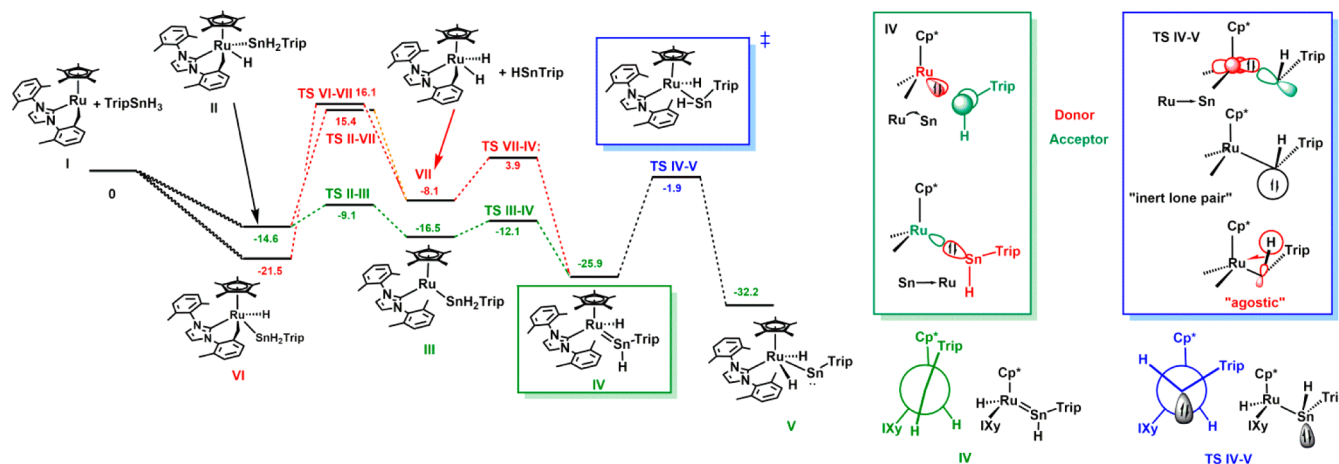


Figure 2. Gibbs free energy profile for the formation of **V**; the insets describe the bonding in **IV** and **TS IV–V**; and Newman projections along Sn–Ru bond of **IV** and **TS IV–V**.

from the SnH_2Trip ligand (activation barrier of $4.4 \text{ kcal mol}^{-1}$ above **III**), to form the 18-electron stannylene complex **IV** with a Gibbs free energy of $-25.9 \text{ kcal mol}^{-1}$ relative to the energy reference. For comparison, C–H reductive elimination in **VI** is energetically less favored and requires deinsertion of the stannylene H–Sn–Trip, followed by reinsertion into a Ru–H bond (Figure 2). This process is associated with a high-energy transition state (TS **VI–VII**).

A related high-energy deinsertion/insertion pathway has also been identified starting from **II**, indicating that **III** is required for the formation of stannylene complex **IV**. This further implicates the formation of **II** and **VI** through the reversible oxidative addition of TripSnH_3 to **I** or through other types of intramolecular isomerization processes; however, the productive generation of **IV** appears to proceed via intermediates **II** and **III**. Note that the silicon congener of **VI**, $\text{Cp}^*(\text{IXy-H})(\text{H})\text{RuSiH}_2\text{Trip}$, was isolated and observed to behave as a “masked silylene” via a process analogous to the conversion of **VI** to **IV**.²⁴

The transformation of **IV** to **V** is exoergic by $6.3 \text{ kcal mol}^{-1}$ and consistent with replacement of a weak Sn–H bond by a stronger Ru–H bond. The transition state for this step (TS **IV–V**) is located $24.0 \text{ kcal mol}^{-1}$ above **IV** and thus is implicated as the rate-determining step for the formation of **V**. This value compares well with the experimental value of 21 kcal mol^{-1} , measured for the first-order transformation of **4** to **5**. In addition, the Gibbs free energy profile of Figure 2 is consistent with the experimental observation of complex **4** (corresponding to **IV**) as the only observable intermediate. The agreement between the experimental KIE of 1.3 and the calculated value of 1.08 further confirms the proposed mechanism.

The optimized structures of **IV** and TS **IV–V** (see Figure 3) are critical for analysis of the mechanism of α -H migration in

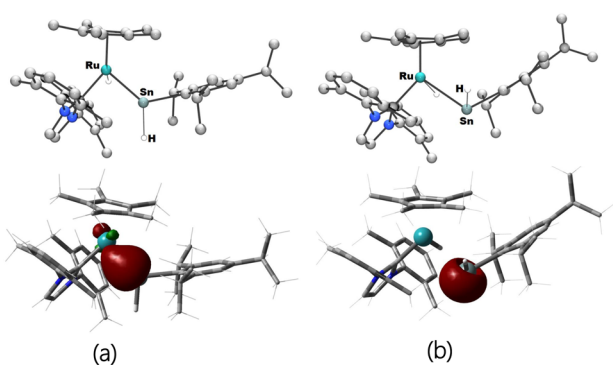


Figure 3. (a) top: the optimized structure of **IV**; bottom: the NLMO showing the σ Sn–Ru bond in **IV** (b) top: the optimized structure of TS **IV–V**; bottom: the NLMO showing the lone pair of Sn in TS **IV–V**.

saturated complex **4**. In **IV**, the Ru–Sn distance is 2.468 \AA , and the Ru–H and Ru–C(NHC) bond lengths are 1.603 and 2.202 \AA , respectively. The tin center is coplanar with its Ru, H, and C_{ipso} substituents (sum of angles at Sn = 358.0°), suggesting σ -donation from an sp^2 lone pair of Sn to Ru, while Ru backdonates into the empty 5p orbital of Sn as known for related carbene complexes.²⁷

In TS **IV–V**, the Ru–Sn distance of 2.837 \AA has elongated relative to those in **IV** and **V** (2.468 and 2.655 \AA , respectively), and the Sn \cdots H distance of 1.802 \AA is significantly longer than that in **IV** (1.762 \AA). An important geometrical change from **IV**

to TS **IV–V** involves a reorientation of the SnHTrip fragment relative to the Ru center. This is quantified by the angles between planes defined by the $\text{Cp}^*_{\text{centroid}}\text{–Ru–Sn}$ and $\text{H–Sn–C}_{\text{ipso}}$ fragments, of 21.3° in **IV** and 70.8° in TS **IV–V**. Also, it can be visualized by Newman projections down the Sn–Ru bonds (Figure 2), which show that the Trip and H substituents on Sn are nearly eclipsed with the Cp^* and IXy ligands for **IV**, whereas a staggered geometry is observed for TS **IV–V**.

This change in orientation of the SnHTrip fragment is associated with a profound modification of the Ru–Sn bonding mode in going from **IV** to TS **IV–V**, as depicted in the orbital interactions derived from an NBO analysis and displayed in Figure 3. Thus, in TS **IV–V**, the original sp^2 lone pair on Sn responsible for σ -donation to Ru becomes strongly localized on Sn with 80% 5s character and negligible interaction with Ru (Figure 3b). This development of greater 5s character in the Sn-based orbital is the result of relativistic effects which are important in heavy elements and lead to an “inert lone pair”.²⁸ The increased s character of the Sn-based lone pair accompanies the dissociation of Sn from Ru at a relatively low-energy cost. Importantly, as the stannylene unit pivots toward its new position in the transition state, the Sn–Ru double bond is replaced by a Ru \rightarrow Sn donor–acceptor interaction. This new interaction makes use of a delocalized, Ru-based orbital that donates into the Sn-based 5p orbital of the stannylene (Figure 2 insets and S1).²⁹ This motion also leads to a strong polarization of the Sn–H bond toward hydrogen (32% Sn and 68% H, according to NBO) and movement of the hydrogen toward the Ru center. Thus, in the transition state there appears to be a weak Ru \cdots HSn interaction as shown by a RuSnH angle of 80.7° and a Ru \cdots H distance of 3.108 \AA . This transition state evolves by full activation of the Sn–H agostic bond to form **V**. Interestingly, this reaction pathway involving a reorientation of a stannylene fragment within a metal’s coordination sphere is reminiscent of the step proposed in the dehydrocoupling of stannanes, involving the metal hydride-stabilized stannylene in the intermediate $\text{Cp}_2(\text{Cl})\text{HfH} \rightarrow \text{SnH}_2$.³⁰

Thus, these experimental and computational results show that α -hydrogen migration in an electronically saturated stannylene complex is possible. It is therefore of interest to compare the Os-based system of eq 1, which undergoes an analogous transformation which is not intramolecular. This dissimilarity may result from the higher energy required to cleave a Os=Sn (vs Ru=Sn) bond. Indeed, DFT calculations reveal that a transition state for the intramolecular α -hydrogen migration in **1**, analogous to TS **IV–V**, is significantly higher in energy ($36.4 \text{ kcal mol}^{-1}$ above **1**). Therefore, this reaction proceeds by an alternate, radical-mediated, pathway.

In summary, we have demonstrated the formation of a ruthenostannylene complex by way of an unusual, intramolecular α -hydrogen migration pathway. This transformation involves a reversal of the role for a coordinated atom, from its usual behavior as an electron donor to that of an acceptor, in a simple molecular motion. This reaction pathway, in maintaining the metal–ligand bonding, lifts the normal requirement for generation of an unsaturated metal center in migration chemistry. This chemistry utilizes a unique property (inert lone pair) of heavier main group atoms and has implications for discovery of new transition metal–main group chemistry.

■ ASSOCIATED CONTENT

📄 Supporting Information

Experimental and computational details. Coordinates of computed structures as a .xyz file. This material is available free of charge via the Internet at <http://pubs.acs.org>.

■ AUTHOR INFORMATION

Corresponding Authors

odile.eisenstein@univ-montp2.fr
tdtilley@berkeley.edu

Notes

The authors declare no competing financial interest.

■ ACKNOWLEDGMENTS

This work was funded by the National Science Foundation under grant no. CHE-1265674. The X-ray Crystallography facility (College of Chemistry, University of California, Berkeley) is supported by the National Science Foundation under grant no. CHE-0840505. C.R. thanks the CNRS and the MENESR for a sabbatical leave at LCT (UPMC, CNRS).

■ REFERENCES

- (1) Cooper, N. J.; Green, M. L. H. *J. Chem. Soc., Dalton Trans.* **1979**, 1121–1127.
- (2) Threlkel, R. S.; Bercaw, J. E. *J. Am. Chem. Soc.* **1981**, *103*, 2650–2659.
- (3) Turner, H. W.; Schrock, R. R.; Fellmann, J. D.; Holmes, S. J. *J. Am. Chem. Soc.* **1983**, *105*, 4942–4950.
- (4) Caulton, K. G. *J. Organomet. Chem.* **2001**, *617–618*, 56–64.
- (5) Luecke, H. F.; Arndtsen, B. A.; Burger, P.; Bergman, R. G. *J. Am. Chem. Soc.* **1996**, *118*, 2517–2518.
- (6) Lee, D.-H.; Chen, J.; Faller, J. W.; Crabtree, R. H. *Chem. Commun.* **2001**, 213–214.
- (7) Alias, F. M.; Poveda, M. L.; Sellin, M.; Carmona, E. *J. Am. Chem. Soc.* **1998**, *120*, 5816–5817.
- (8) Empsall, H. D.; Hyde, E. M.; Markham, R.; McDonald, W. S.; Norton, M. C.; Shaw, B. L.; Weeks, B. J. *Chem. Soc., Chem. Commun.* **1977**, 589–590.
- (9) Grubbs, R. H.; Coates, G. W. *Acc. Chem. Res.* **1996**, *29*, 85–93.
- (10) Mitchell, G. P.; Tilley, T. D. *Angew. Chem., Int. Ed.* **1998**, *37*, 2524–2526.
- (11) Glaser, P. B.; Tilley, T. D. *J. Am. Chem. Soc.* **2003**, *125*, 13640–13641.
- (12) Hayes, P. G.; Beddie, C.; Hall, M. B.; Waterman, R.; Tilley, T. D. *J. Am. Chem. Soc.* **2006**, *128*, 428–429.
- (13) Waterman, R.; Hayes, P. G.; Tilley, T. D. *Acc. Chem. Res.* **2007**, *40*, 712–719.
- (14) Hayes, P. G.; Waterman, R.; Glaser, P. B.; Tilley, T. D. *Organometallics* **2009**, *28*, 5082–5089.
- (15) Shinohara, A.; McBee, J.; Tilley, T. D. *Inorg. Chem.* **2009**, *48*, 8081–8083.
- (16) Fasulo, M. E.; Tilley, T. D. *Chem. Commun.* **2012**, *48*, 7690–7692.
- (17) Hayes, P. G.; Gribble, C. W.; Waterman, R.; Tilley, T. D. *J. Am. Chem. Soc.* **2009**, *131*, 4606–4607.
- (18) Pu, L.; Twamley, B.; Haubrich, S. T.; Olmstead, M. M.; Mork, B. V.; Simons, R. S.; Power, P. P. *J. Am. Chem. Soc.* **2000**, *122*, 650–656.
- (19) Eichler, B. E.; Phillips, A. D.; Haubrich, S. T.; Mork, B. V.; Power, P. P. *Organometallics* **2002**, *21*, 5622–5627.
- (20) Jutzi, P.; Leue, C. *Organometallics* **1994**, *13*, 2898–2899.
- (21) Inoue, S.; Driess, M. *Organometallics* **2009**, *28*, 5032–5035.
- (22) Lei, H.; Guo, J.-D.; Fettingner, J. C.; Nagase, S.; Power, P. P. *Organometallics* **2011**, *30*, 6316–6322.
- (23) Stewart, M. A.; Moore, C. E.; Ditri, T. B.; Labios, L. A.; Rheingold, A. L.; Figueroa, J. S. *Chem. Commun.* **2011**, *47*, 406–408.

(24) Liu, H.-J.; Raynaud, C.; Eisenstein, O.; Tilley, T. D. *J. Am. Chem. Soc.* **2014**, *136*, 11473–11482.

(25) Pandey, K. K.; Power, P. P. *Organometallics* **2011**, *30*, 3353–3361.

(26) PBE0 functional, corrected for dispersion as proposed by Grimme (D3 correction, BJ damping), with the def2-TZVPP basis set for all atoms and quasi-relativistic ECP for Sn and Ru was used. Solvent effects (benzene) were included by means of SMD (see SI for full computational details).

(27) (a) Schilling, B. E. R.; Hoffmann, R.; Faller, J. W. *J. Am. Chem. Soc.* **1979**, *101*, 592–598. (b) Schilling, B. E. R.; Hoffmann, R.; Lichtenberger, D. L. *J. Am. Chem. Soc.* **1979**, *101*, 585–591.

(28) (a) Pyykkö, P. *Chem. Rev.* **1988**, *88*, 563–594. (b) Power, P. P. *Chem. Rev.* **1999**, *99*, 3463–3504.

(29) The delocalized Ru-base orbital includes the Ru lone pair, Ru–H and Ru–C(NHC) bonding orbitals.

(30) Guilhaumé, J.; Raynaud, C.; Eisenstein, O.; Perrin, L.; Maron, L.; Tilley, T. D. *Angew. Chem., Int. Ed.* **2010**, *49*, 1816–1819.